Selectivity switch between FAK and Pyk2: Macrocyclization of FAK inhibitors improves Pyk2 potency

Julie Farand, Nicholas Mai, Jayaraman Chandrasekhar, Zachary E. Newby, Josh Van Veldhuizen, Jennifer Loyer-Drew, Chandrasekar Venkataramani, Juan Guerrero, Amy Kwok, Ning Li, Yelena Zherebina, Sibylle Wilbert, Jeff Zablocki, Gary Phillips, William J. Watkins, Robert Mourey, Gregory Notte

PII: S0960-894X(16)31140-4
DOI: http://dx.doi.org/10.1016/j.bmcl.2016.10.092
Reference: BMCL 24395

To appear in: *Bioorganic & Medicinal Chemistry Letters*

Received Date: 30 September 2016
Revised Date: 30 October 2016
Accepted Date: 31 October 2016

Please cite this article as: Farand, J., Mai, N., Chandrasekhar, J., Newby, Z.E., Van Veldhuizen, J., Loyer-Drew, J., Venkataramani, C., Guerrero, J., Kwok, A., Li, N., Zherebina, Y., Wilbert, S., Zablocki, J., Phillips, G., Watkins, W.J., Mourey, R., Notte, G., Selectivity switch between FAK and Pyk2: Macrocyclization of FAK inhibitors improves Pyk2 potency, *Bioorganic & Medicinal Chemistry Letters* (2016), doi: http://dx.doi.org/10.1016/j.bmcl.2016.10.092

Bioorganic & Medicinal Chemistry Letters
journal homepage: www.elsevier.com

Selectivity switch between FAK and Pyk2: macrocyclization of FAK inhibitors improves Pyk2 potency

Julie Farand [a,*], Nicholas Mai [a], Jayaraman Chandrasekhar [e], Zachary E. Newby [b], Josh Van Veldhuizen [d], Jennifer Loyer-Drew [d], Chandrasekar Venkataramani [a], Juan Guerrero [a], Amy Kwok [c], Ning Li [c], Yelena Zherebina [c], Sibylle Wilbert [f], Jeff Zablocki [a], Gary Phillips [d], William J. Watkins [a], Robert Mourey [g], Gregory Notte [a]

[a]*Department of Medicinal Chemistry,* [b]*Department of Structural Chemistry and* [c]*Department of Biology, Gilead Sciences, Inc., 333 Lakeside Drive, Foster City, CA 94404, USA*
[d]*Department of Medicinal Chemistry,* [e]*Department of Structural Chemistry,* [f]*Department of Drug Metabolism and* [g]*Department of Biology, Gilead Sciences, Inc., 199 East Blaine Street, Seattle, WA 98102, USA*

ARTICLE INFO

Article history:
Received
Revised
Accepted
Available online

Keywords:
Pyk2
FAK
Macrocycle
Atropisomer
Glioblastoma

ABSTRACT

Herein, we describe the synthesis of Pyk2 inhibitors via macrocyclization of FAK and dual Pyk2-FAK inhibitors. We identified macrocycle **25a** as a highly potent Pyk2 inhibitor (IC_{50} = 0.7 nM), with ~175-fold improvement in Pyk2 potency as compared to its acyclic counterpart. In many cases, macrocyclization improved Pyk2 potency while weakening FAK potency, thereby improving the Pyk2/FAK selectivity ratio for this structural class of inhibitors. Various macrocyclic linkers were studied in an attempt to optimize Pyk2 selectivity. We observed macrocyclic atropisomerism during the synthesis of 19-membered macrocycles **10a-d**, and successfully obtained crystallographic evidence of one atropisomer (**10a-AtropB**) preferentially bound to Pyk2.

Proline-rich tyrosine kinase 2 (Pyk2) is a non-receptor cytoplasmic tyrosine kinase within the focal adhesion kinase (FAK) subfamily. Both Pyk2 and FAK are involved in multiple signaling pathways that regulate cell migration, proliferation and survival.[1,2] Over the last decade, genetic knockdown of Pyk2 together with inhibition by small molecules have demonstrated the potential role of Pyk2 in the treatment of osteoporosis.[3,4] Recently, the biological significance of the focal adhesion kinases in promoting the migration and invasion of malignant cells has been of increasing interest.[5,6,7] Glioblastoma multiforme is the most common and most aggressive malignant primary brain tumor due to the propensity of peripheral glioma cells to migrate and disperse among neighboring normal brain cells. Combinations of surgical resection, radiotherapy and/or chemotherapy with temozolomide are not curative treatments. Over 90% of the estimated new glioblastoma cases in 2015 were found in adults ≥40 years old. The 5-year relative survival rate for patients diagnosed with glioblastoma is 5.1%, a statistic which has shown no significant improvement over the past 30 years, in spite of recent therapeutic advancements.[8] Given this unmet medical need, we sought to selectively target Pyk2 and evaluate its role in the migration and invasion of malignant glioblastoma cells. Unlike FAK, which is ubiquitously expressed, Pyk2 expression is highly localized in the brain, hematopoietic and nervous systems.[9,10] Radial migration assays using SF767 glioblastoma cell lines have shown upregulation of

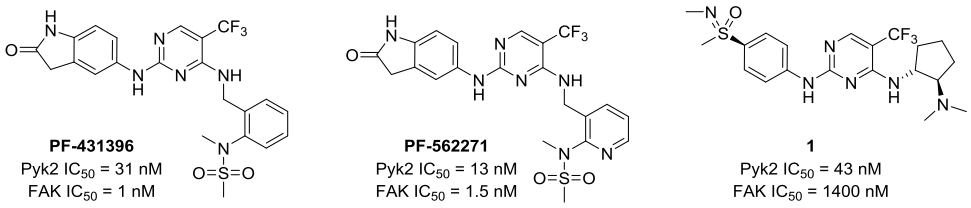

Figure 1. Representative structures of reported diaminopyrimidine Pyk2/FAK inhibitors.

* Corresponding author. Tel.: +1-650-372-7668; e-mail: Julie.Farand@gilead.com

Pyk2 in cells at the migratory rim relative to those at the primary core.[11] A direct correlation between the rate of migration and levels of activated Pyk2 was also observed. Conversely, silencing Pyk2 expression with siRNA significantly reduced the migratory potential of glioblastoma cells.[12] A relationship has also been demonstrated between increasing Pyk2 expression/phosphorylation events and advancing tumor WHO grade, thus indicating Pyk2 as a potential mediator of glioblastoma progression.[13]

The catalytic domains of Pyk2 and FAK kinases have 73% sequence similarity. The similarity is slightly higher (78%) for residues generally thought to form the ATP binding sites of these two enzymes.[14] Consequently, the discovery of a small molecule inhibitor selective for Pyk2 has been challenging. We initiated efforts toward that goal for proof-of-concept studies and focused our attention on diaminopyrimidine-based inhibitors **PF-431396**[3,15], **PF-562271**[16] and compound **1**[17] (Figure 1). **PF-562271** was described as a potent, ATP-competitive and reversible FAK inhibitor (IC_{50} = 1.5 nM) with a ~9-fold selectivity over Pyk2 (IC_{50} = 13 nM). To better understand the interaction of **PF-562271** with Pyk2, we solved a crystal structure of the complex. A comparison in the binding pose of **PF-562271** complexed with FAK[18] versus Pyk2[19] revealed a significant conformational difference in the amino-methyl pyridinyl sulfonamide group (Figures 2a and 2b). The rotamer of the benzylic CH_2-NH bond of **PF-562271** observed in the Pyk2-bound structure induced a conformation of the nearby DFG loop in Pyk2 (DFG-in) distinct from that observed in FAK (helical DFG). We hypothesized that a macrocyclic analogue of **PF-562271** favoring the Pyk2-bound conformation shown in Figure 2b would enhance selectivity of the inhibitor over FAK.[20]

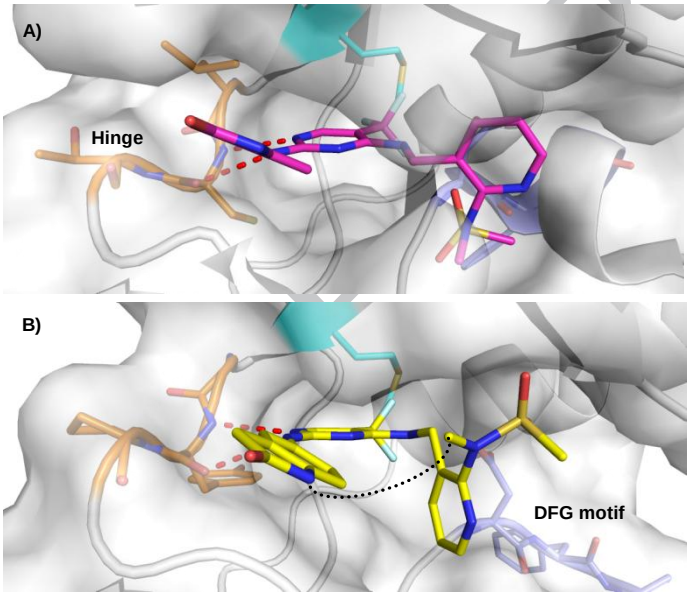

Figure 2. (A) Co-crystal structure of **PF-562271** (pink) bound to FAK (PDB entry 3BZ3)[18] showing the methionine gatekeeper (cyan), the hydrogen bonding interactions between the aminopyrimidine and the hinge backbone (orange), as well as the amino-methyl pyridinyl sulfonamide group projecting toward the DFG motif (residues Asp-Phe-Gly in lavender). (B) Co-crystal structure of **PF-562271** (yellow) bound to Pyk2 (PDB entry 5TOB, resolution 2.2 Å) depicting the amino-methyl pyridinyl sulfonamide group adopting a unique conformation next to the DFG motif. The macrocyclization strategy is also depicted (black dotted line).

Macrocycle **10a** was synthesized as described in Schemes 1 and 2. Under S_NAr conditions, 2-chloronicotinonitrile **2a** was heated with *tert*-butyl 5-aminopentanoate in refluxing ethanol (Scheme 1).[21] The resulting aminopyridine was treated with mesyl chloride and the nitrile was subsequently reduced to afford amine **3a**. Chloroaminopyrimidine intermediate **7** was heated with **3a** under basic conditions to generate diaminopyrimidine **8a** (Scheme 2).[15,22] Following *N*-Boc deprotection and *tert*-butyl ester hydrolysis, crude amino acid **9a** was subjected to a HATU-mediated macrolactamization under dilute conditions to provide **10a** in 56% yield over two steps.[23] In contrast to **PF-562271**, **10a** exhibited moderate selectivity for Pyk2 over FAK (Pyk2 IC_{50} = 3.1 nM, FAK IC_{50} = 17 nM, Table 1) demonstrating the validity of the macrocyclization strategy. The excellent cellular permeability of **10a** was also notable (Caco-2: A to B = 30 x 10^{-6} cm/s and B to A = 32 x 10^{-6} cm/s) and displayed a moderate improvement over acyclic inhibitor **PF-562271** in the absorptive direction (Caco-2: A to B = 11 x 10^{-6} cm/s and B to A = 29 x 10^{-6} cm/s).

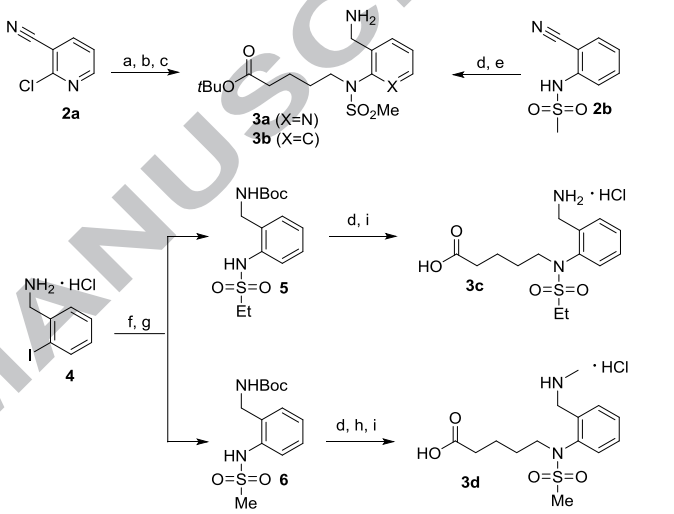

Scheme 1. Reagents and conditions for *N*-pyridinylmethanesulfonamide and *N*-phenylsulfonamides: (a) $tBuO_2C(CH_2)_4NH_2$, EtOH, 85°C (54%); (b) LiHMDS, MsCl, THF, -78°C (64%): (c) H_2, Raney Ni, 50 bar, EtOH, 60°C (40%); (d) $Br(CH_2)_4CO_2tBu$, K_2CO_3, DMF, 125°C (54-82%)[24]; (e) H_2, Raney Ni, 70 bar, EtOH, 50°C (50%); (f) Boc_2O, $NaHCO_3$, THF/H_2O (95%); (g) $MeSO_2NH_2$ or $EtSO_2NH_2$, CuI, *N*-methylglycine, K_3PO_4, DMF, 100°C (40%); (h) NaH, MeI, THF (85%); (i) 4N HCl in 1,4-dioxane (95%).

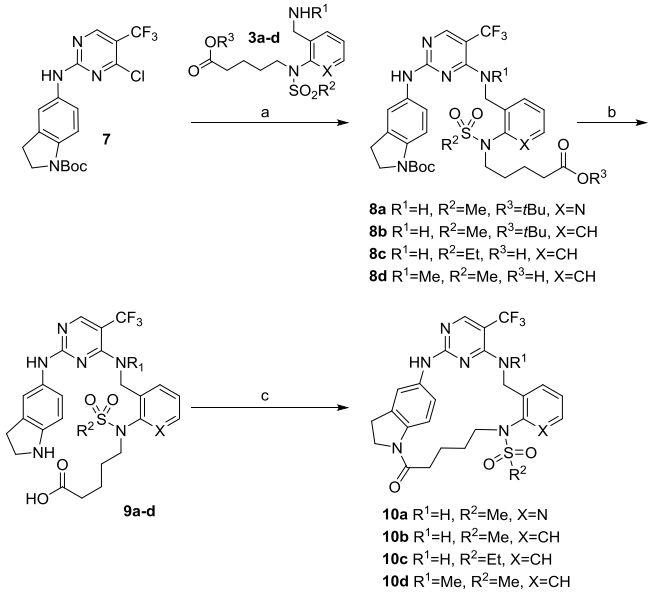

Scheme 2. Reagents and conditions: (a) iPr_2NH, PhMe/IPA, 90°C; (b) TFA, DCM; (c) HATU, 4-methylmorpholine, DMF (0.005M) (10-30% over 3 steps).

Interestingly, a small molecule crystal structure of **10a** revealed the presence of atropisomers **10a-AtropA** and **10a-AtropB** in the solid state (Figure 3a).[25] For **10a-AtropA**, the linker alkyl chain appeared disordered but was successfully modeled as 80/20 occupancy. Co-crystallization of macrocycle **10a** with Pyk2 confirmed preservation of the binding mode, inhibitor conformation, protein-inhibitor interactions and revealed the kinase adopting a DFG-in conformation (Figure 3b).[26] An overlay of the Pyk2-bound conformation of **10a** with the solid state conformation of **10a-AtropB** indicated that the latter was the relevant atropisomer for inhibition (Figure 3c). Attempts to separate the atropisomers in chiral HPLC and SFC screens were unsuccessful, suggesting that rapid interconversion was occurring on the HPLC timescale.[27,28] On the other hand, chiral HPLC analysis of the *N*-phenylmethanesulfonamide macrocycle **10b** (Pyk2 IC_{50} = 0.9 nM) suggested a 1:1 ratio of atropisomers, however baseline resolution of the split peak could not be achieved, presumably due to on-column interconversion.[29]

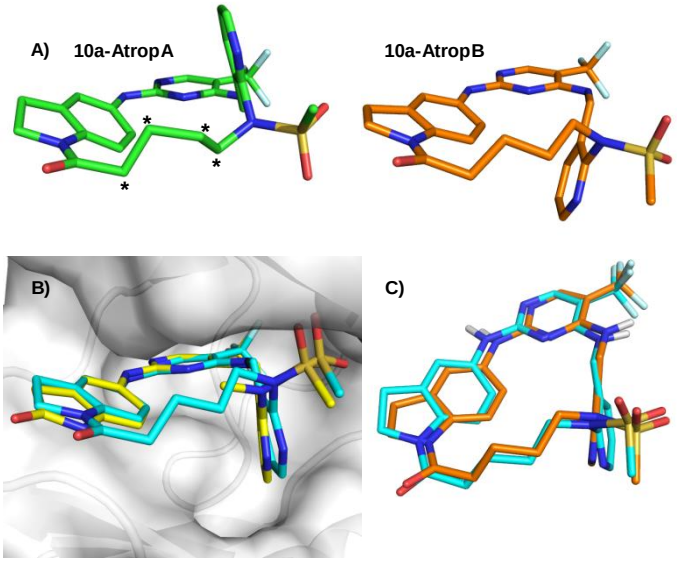

Figure 3. (A) Small molecule X-ray structure (0.75 Å) of macrocycle **10a** as a mixture of atropisomers **10a-AtropA** (green) and **10a-AtropB** (orange). Atoms disordered in the crystal are labeled with an asterisk (*). (B) Co-crystal structure overlay of macrocycle **10a** (cyan, PDB entry 5TO8, resolution 2.0 Å) and **PF-562271** (yellow) bound to Pyk2. (C) Overlay of macrocycle **10a** (cyan) bound to Pyk2 and small molecule X-ray structure of **10a-AtropB** (orange).

To increase the energy barrier for atropisomer interconversion, we focused our attention on *N*-phenylsulfonamides, prepared the bulkier ethyl sulfonamide **10c**, and also explored the effect of alkylation of the secondary benzylic amine in the form of the tertiary analogue **10d**. 1-Iodobenzylamine hydrochloride **4** proved useful as a starting material for both compounds, with copper mediated *N*-arylation of the sulfonamide[30] and selective alkylation of the sulfonamide over the carbamate under basic conditions as key steps (Scheme 1). Chiral HPLC analysis of **10c** and **10d** were qualitatively similar and showed two peaks separated by a plateau, which suggested the atropisomers may be separable on preparative scale.[27,31] Unfortunately, however, peak resolution for **10c** could not be achieved due to on-column interconversion. Nonetheless, the rapidly interconverting class 1 atropisomers[32] constituting both **10c** and **10d** showed >100-fold improvement in Pyk2 IC_{50} (1.5 nM and 1.9 nM respectively) when compared to their corresponding acyclic diaminopyrimidines **9c** and **9d**, together with 5-fold selectivity over the FAK enzyme (Table 1).

Table 1. Pyk2 and FAK IC_{50} values for diaminopyrimidine macrocycles and acyclic precursors.

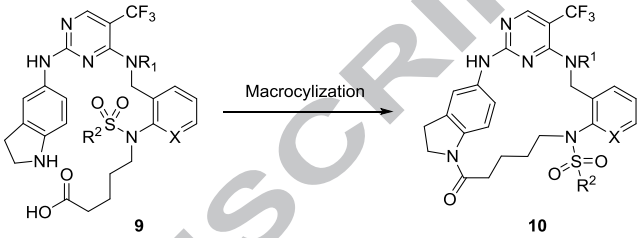

Compound	R^1	R^2	X	Pyk2 IC_{50} (nM)	FAK IC_{50} (nM)
10a	H	Me	N	3.1	17
10b	H	Me	CH	0.9	3.2
9c	H	Et	CH	256	3.3
10c	H	Et	CH	1.9	9.2
9d	Me	Me	CH	201	177
10d	Me	Me	CH	1.5	8.6

The effect of various macrocycle linkers on Pyk2 and FAK biochemical potencies was also investigated (Figure 4). Shortening the 5-carbon linker of **10a** to four carbons yielded **11** as an 18-membered macrocyclic dual Pyk2/FAK inhibitor with a 10-fold loss in Pyk2 potency (IC_{50} = 30 nM). Replacing the tertiary methyl sulfonamide moiety in **10b** with a secondary sulfonamide within the linker afforded 19-membered macrocycle **12**, an equipotent Pyk2 inhibitor (IC_{50} = 3.5 nM) with a slight erosion in FAK selectivity compared to **10b**.[33] Rigidifying macrocycle **13** with a phenyl-containing linker did not improve selectivity.

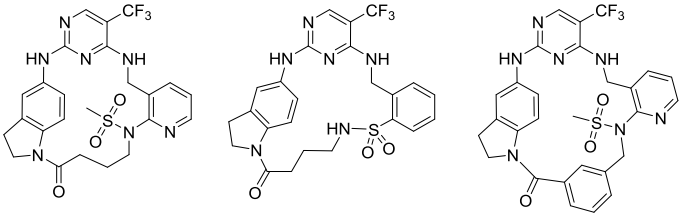

Figure 4. Effect of various linkers on Pyk2 and FAK potencies.

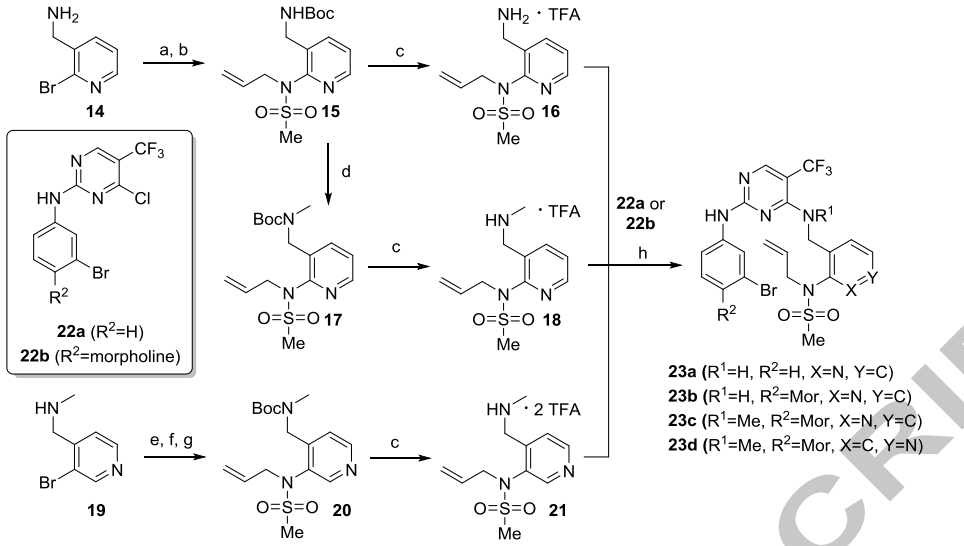

Scheme 3. Reagents and conditions: (a) Boc_2O, Et_3N, CH_2Cl_2 (90%); (b) (Allyl)$NHSO_2Me$, CuI, DMEDA, K_2CO_3, ACN, 70°C (74%)[34]; (c) TFA/DCM (58%-quantitative); (d) NaH, MeI, THF (98%); (e) Boc_2O, $NaHCO_3$, THF/H_2O (91%); (f) $MeSO_2NH_2$, CuI, 1,3-di(2-pyridyl)-1,3-propanedione, K_2CO_3, DMF, 120°C (89%); (g) AllylBr, K_2CO_3, ACN, 70°C (66%); (h) **22a** or **22b**, iPr_2NH, PhMe/IPA, 90°C (38-75%).[15]

Table 2. Intrinsic potencies for acyclic and 15-membered macrocyclic diaminopyrimidines.

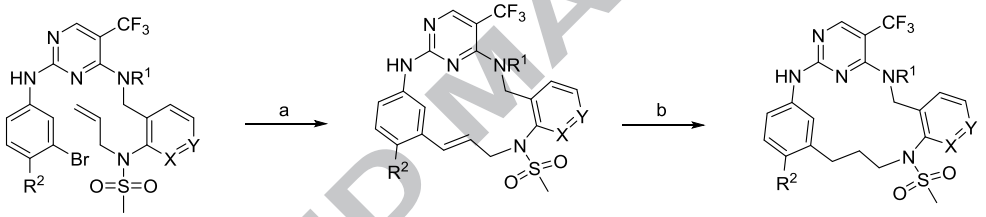

Compound	R^1	R^2	X	Y	Pyk2 IC_{50} (nM)	FAK IC_{50} (nM)
23a	H	H	N	CH	122	0.51
24a	H	H	N	CH	2.60	10.2
25a	H	H	N	CH	0.67	1.26
23b	H	Morpholine	N	CH	19.5	0.51
24b	H	Morpholine	N	CH	0.84	4.34
25b	H	Morpholine	N	CH	1.31	3.21
24c	Me	Morpholine	N	CH	1.55	5.75
23d	Me	Morpholine	CH	N	6625	7496
24d	Me	Morpholine	CH	N	2.70	14.0

(a) For **24a-c**: $Pd(OAc)_2$, (tBu)$_3$P, Et_3N, ACN, 80°C (14-31%); and for **24d**: $Pd_2(dba)_3$, (tBu)$_3$P, Cy_2NMe, 1,4-dioxane, 90°C (10%); (b) H_2, Pd/C, EtOH/EtOAc (50-67%).

N-Phenylsulfonamide macrocycles **10b-d** suffered from poor solubility (<1.6 µM at pH 7), and short half-lives were observed for **10a-d** in mouse, dog and/or human liver microsomes ($t_{1/2}$ < 60 min). For the next generation of macrocyclic Pyk2 inhibitors, we employed an intramolecular Heck reaction for the ring closure step. Macrocycles with morpholine as R^2 and/or 3-pyridyl regioisomers were prepared as a tactic to enhance solubility (Scheme 3). Intermediate **20**, used as a precursor for the synthesis of macrocycle **23d**, was prepared via a copper-catalyzed *N*-arylation of methanesulfonamide.[35] Heck-mediated macrocyclizations of **23a-d** under dilute conditions provided inhibitors **24a-d** bearing 3-carbon linkers, thus decreasing the number of sites for potential metabolism (Table 2). In some cases, the alkene was reduced with Pd/C under an atmosphere of hydrogen to yield macrocycles **25a** and **25b**. Assessment of the activities of the acyclic precursors **23a-b** relative to the macrocycles **24a-b** proved further evidence of the potency switch toward Pyk2 and selectivity improvement in the latter. Strikingly, the acyclic tertiary amine **23d** was markedly less active against both enzymes but macrocyclization to **24d** provided for ~2,500-fold and 500-fold increases in potency against Pyk2 and FAK respectively. Saturation of the macrocyclic linker in **25a** led to a modest improvement in Pyk2 potency, albeit with a relative loss in selectivity. Incremental improvements in kinetic solubility at physiological pH were noticed between **24a**, **24c** and **24d** (0.3, 1 and 3 µM respectively). Macrocycle **24d,** bearing an unsaturated 3-carbon linker, exemplified the most metabolically stable analogue tested in the human microsomal stability assay ($t_{1/2}$ = 263 min).

Conformational analysis provides further insight into the SAR trends apparent in Table 2. Acyclic precursors **23a-b** are 25-50 fold less active than their macrocyclic counterparts **24a-b** against Pyk2. The global minima for **23a-b** are conformations in which the $–NHCH_2$- linker between the pyrimidine and pyridine rings is staggered, and the calculated energy penalty to adopt the gauche local minima evident in the bioactive conformation (cf Figure 3c) is ca. 2.3 kcal/mol.[36] In the still more dramatic case of the tertiary amines, the 2,500-fold Pyk2 potency differential is largely explained by the same phenomenon coupled with the need for the N-Me substituent to lie in the same plane and pointing towards the adjacent *o*-CF_3 substituent – a conformation that lies 4.3 kcal/mol above the global minimum for the acyclic analogue **23d**. Conformational analysis also confirms that second generation macrocycles **24a**, **24d** and **25a** can adopt a low energy conformation (either the global minimum or within 0.5 kcal/mol of it) that overlays closely with the small molecule crystal structure of **10a-AtropB** (Figure 4). The detrimental conformational effect of *N*-methylation is effectively overcome through macrocyclization of **23d** to **24d**.

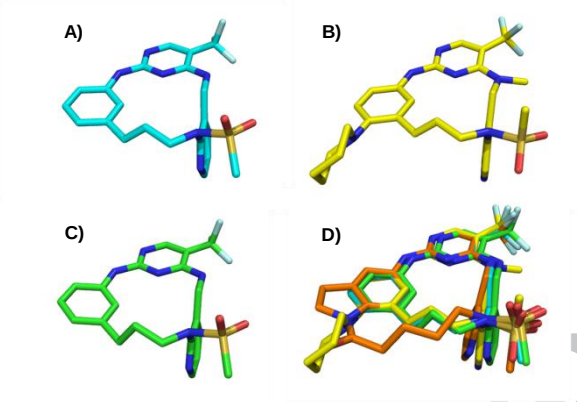

Figure 4. Calculated low energy conformations of second generation macrocycles (A) with secondary benzylic amine **24a** (cyan), (B) tertiary benzylic amine **24d** (yellow) and (C) highly potent Pyk2 inhibitor **25a** bearing a saturated linker (green). (D) Overlay of the minimized conformations of **24a**, **24d** and **25a** with the small molecule crystal structure **10a-AtropB** (orange).

In summary, the use of a macrocyclization strategy provided an enhancement in Pyk2 vs FAK selectivity, despite the high degree of sequence similarity in their active sites. Macrocyclic atropisomerism was observed with **10a**, where the solid state conformation of **10a-AtropB** was found to be remarkably similar to the Pyk2 bound conformation. The excellent *in vitro* potencies of macrocycles **10**, **12**, **24** and **25** (IC_{50} = 0.7 - 3.1 nM), combined with their Pyk2/FAK selectivity (2- to 3-fold), render them suitable tool compounds for future proof-of-concept studies. Improving solubility, metabolic stability and ensuring blood brain barrier permeability will be necessary to enable their utility in glioblastoma xenograft models.

Acknowledgments

The authors wish to thank Professor Arnold L. Rheingold for providing small molecule X-ray crystallography data, and we appreciate insightful discussions with Richard Neve during the review of this manuscript.

References and Notes

1. Schlaepfer, D. D.; Hauck, C. R.; Sieg, D. J. *Prog. Biophys. Mol. Bio.* **1999**, *71*, 435.
2. Parsons, J. T. *J. Cell Sci.* **2003**, *116*, 1409.
3. Buckbinder, L.; Crawford, D. T.; Qi, H.; Ke, H.-Z.; Olson, L. M.; Long, K. R.; Bonnette, P. C.; Baumann, A. P.; Hambor, J. E.; Grasser, W. A.; Pan, L. C.; Owen, T. A.; Luzzio, M. J.; Hulford, C. A.; Gebhard, D. F.; Paralkar, V. M.; Simmons, H. A.; Kath, J. C.; Roberts, W. G.; Smock, S. L.; Guzman-Perez, A.; Brown, T. A.; Li, M. *Proc. Natl. Acad. Sci. U.S.A.* **2007**, *104*, 10619.
4. Allen, J. G.; Lee, M. R.; Han, C.-Y. E.; Scherrer, J.; Flynn, S.; Boucher, C.; Zhao, H.; O'Connor, A. B.; Roveto, P.; Bauer, D.; Graceffa, R.; Richards, W. G.; Babij, P. *Bioorg. Med. Chem. Lett.* **2009**, *19*, 4924.
5. Lipinski, C. A.; Loftus, J. C. *Expert Opin. Ther. Targets* **2010**, *14*, 95.
6. Schultze, A.; Fiedler, W. *Expert Opin. Investig. Drugs* **2010**, *19*, 777.
7. Fan, H.; Guan, J.-L. *J. Biol. Chem.* **2011**, *286*, 18573.
8. Ostrom, Q. T.; Gittleman, H.; Fulop, J.; Liu, M.; Blanda, R.; Kromer, C.; Wolinsky, Y.; Kruchko, C.; Barnholtz-Sloan, J. S. *Neuro. Oncol.* **2015**, *17*, iv1.
9. Lev, S.; Moreno, H.; Martinez, R.; Canoli, P.; Peles, E.; Musacchio, J. M.; Plowman, G. D.; Rugy, B.; Schlessinger, J. *Nature* **1995**, *376*, 737.
10. Avraham, S.; London, R.; Fu, Y.; Ota, S.; Hiregowdara, D.; Li, J.; Jiang, S.; Pasztor, L. M.; White, R. A.; Groopman, J. E.; Avraham, H. *J. Biol. Chem.* **1995**, *270*, 27742.
11. Lipinski, C. A.; Tran, N. L.; Bay, C.; Kloss, J.; McDonough, W. S.; Beaudry, C.; Berens, M. E.; Loftus, J. C. *Mol. Cancer Res.* **2003**, *1*, 323.
12. Lipinski, C. A.; Tran, N. L.; Menashi, E.; Rohl, C.; Kloss, J.; Bay, R. C.; Berens, M. E.; Loftus, J. C. *Neoplasia* **2005**, *7*, 435.
13. Gutenberg, A.; Bruck, W.; Buchfelder, M.; Ludwig, H. C. *Acta Neuropathol.* **2004**, *108*, 224.
14. Xing, L.; Rai, B.; Lunney, E. A. *J. Comput. Aided Mol. Des.* **2014**, *28*, 13.
15. (a) Walker, D. P.; Bi, F. C.; Kalgutkar, A. S.; Bauman, J. N.; Zhao, S. X.; Soglia, J. R.; Aspnes, G. E.; Kung, D. W.; Klug-McLeod, J.; Zawistoski, M. P.; McGlynn, M. A.; Oliver, R.; Dunn, M.; Li, J.-C.; Richter, D. T.; Cooper, B. A.; Kath, J. C.; Hulford, C. A.; Autry, C. L.; Luzzio, M. J.; Ung, E. J.; Roberts, W. G.; Bonnette, P. C.; Buckbinder, L.; Mistry, A.; Griffor, M. C.; Han, S.; Guzman-Perez, A. *Bioorg. Med. Chem. Lett.* **2008**, *18*, 6071; (b) Han, S.; Mistry, A.; Chang, J. S.; Cunningham, D.; Griffor, M.; Bonnette, P. C.; Wang, H.; Chrunyk, B. A.; Aspnes, G. E.; Walker, D. P.; Brosius, A. D.; Buckbinder, L. *J. Biol. Chem.* **2009**, *284*, 13193.
16. Roberts, W. G.; Ung, E.; Whalen, P.; Cooper, B.; Hulford, C.; Autry, C.; Richter, D.; Emerson, E.; Lin, J.; Kath, J.; Coleman, K.; Yao, L.; Martinez-Alsina, L.; Lorenzen, M.; Berliner, M.; Luzzio, M.; Patel, N.; Schmitt, E.; LaGreca, S.; Jani, J.; Wessel, M.; Marr, E.; Griffor, M.; Vajdos, F. *Cancer Res.* **2008**, *68*, 1935.
17. Walker, D. P.; Zawistoski, M. P.; McGlynn, M. A.; Li, J.-C.; Kung, D. W.; Bonnette, P. C.; Baumann, A.; Buckbinder, L.; Houser, J. A.; Boer, J.; Mistry, A.; Han, S.; Xing, L.; Guzman-Perez. *Bioorg. Med. Chem. Lett.* **2009**, *19*, 3253.
18. PDB entry 3BZ3 (2.2 Å): Vajdos, F.; Marr, E.
19. Crystallographic data of **PF-562271** bound to Pyk2 has been deposited to the Protein Data Bank (PDB entry 5TOB, resolution 2.2 Å).
20. Conformational control of small molecule inhibitors via macrocyclization is a well established strategy. For examples, see Johnson, T. W.; Richardson, P. F.; Bailey, S.; Brooun, A.; Burke, J. B.; Collins, M. R.; Cui, J. J.; Deal, J. G.; Deng, Y.-L.; Dinh, D.; Engstrom, L. D.; He, M.; Hoffman, J.; Hoffman, R. L.; Huang, Q.; Kania, R. S.; Kath, J. C.; Lam, H.; Lam, J. L.; Le, P. T.; Lingardo, L.; Liu, W.; McTigue, M.; Palmer, C. L.; Sach, N. W.; Smeal, T.; Smith, G. L.; Stewart, A. E.; Timofeevski, S.; Zhu, H.; Zhu, J.; Zou, H. Y.; Edwards, M. P. *J. Med. Chem.* **2014**, 57, 4720 and references 33 therein.
21. *Tert*-butyl 5-aminopentanoate was prepared and used *in situ* via reductive deprotection of readily available *tert*-butyl 5-(((benzyloxy)carbonyl)amino)pentanoate.
22. For the synthesis of chloroaminopyrimidines and the regioselective addition of anilines to the 2-position of 2,4-dichloro-5-trifluoromethylpyrimidine, see Kath, J. C.; Richter, D. T.; Luzzio, M. J. US Patent 7,122,670, October 16, 2006.
23. ^{1}H NMR (400 MHz, Acetonitrile-d_3) δ 11.08 (s, 1H), 8.44 (dd, *J* = 4.8, 1.8 Hz, 1H), 8.29 (s, 1H), 7.58 – 7.45 (m, 2H), 7.37 (dd, *J* = 7.8, 4.7 Hz, 1H), 7.05 – 6.86 (m, 3H), 4.79 (s, 1H), 4.68 (dd, *J* = 16.9, 5.0 Hz, 1H), 3.99 (t, *J* = 8.2 Hz, 2H), 3.84 – 3.73 (m, 1H), 3.17 – 3.01 (m, 4H), 2.97 – 2.81 (m, 1H), 2.82 – 2.66 (m, 2H),

2.58 – 2.47 (m, 1H), 1.63 – 1.32 (m, 4H). LC-MS (ESI^+) *m/z*: calcd $C_{25}H_{26}F_3N_7O_3S$ (M+H) 562.2, found 562.2 (M+H).
24. For the synthesis of *tert*-butyl 5-bromopentanoate, see Riva, R.; Banfi, L.; Basso, A.; Zito, P. *Org. Biomol. Chem.* **2011**, *9*, 2107.
25. CCDC 1505469 contains the supplementary small molecule crystallographic data. The data can be obtained free of charge from The Cambridge Crystallographic Data Centre via www.ccdc.cam.ac.uk/structures.
26. Crystallographic data of macrocycle **10a** bound to Pyk2 has been deposited to the Protein Data Bank (PDB entry 5TO8, resolution 2.0 Å).
27. Welch, C. J.; Gong, X.; Schafer, W.; Chobanian, H.; Lin, L.; Biba, M.; Liu, P.; Guo, Y.; Beard, A. *Chirality* **2009**, *21*, E105.
28. Elleraas, J.; Ewanicki, J.; Johnson, T. W.; Sach, N. W.; Collins, M. R.; Richardson, P. A. *Angew. Chem. Int. Ed.* **2016**, *55*, 3590.
29. Atropisomers of macrocycle **10b** were detected using a Chiralpak IC analytical chiral column (250 mm x 4.6 mm, particle size 5.0 µm) with 1:1 MeOH/EtOH.
30. Deng, W.; Liu, L.; Zhang, C.; Liu, M.; Guo, Q.-X. *Tetrahedron Lett.* **2005**, *46*, 7295.
31. Atropisomer peaks separated by a plateau were detected with macrocycles **10c** and **10d** using a Chiralcel AZ-H analytical column (250 mm x 4.6 mm, particle size 5.0 µm) with 1:1 MeOH/EtOH.
32. LaPlante, S. R.; Fader, L. D.; Fandrick, K. R.; Fandrick, D. R.; Hucke, O.; Kemper, R.; Miller, S. P. F.; Edwards, P. J. *J. Med. Chem.* **2011**, *54*, 7005.
33. Macrocycle **12** was prepared in a similar fashion to **10b.** Reaction between 2-cyanobenzenesulfonyl chloride and *tert*-butyl γ-aminobutyrate hydrochloride was performed according to Biron, E.; Kessler, H. *J. Org. Chem.* **2005**, *70*, 5183. The nitrile was subsequently reduced using H_2, Raney Ni and EtOH at 70°C (70 bar).
34. Wang, X.; Guram, A.; Ronk, M.; Milne, J. E.; Tedrow, J. S.; Faul, M. M. *Tetrahedron Lett.* **2012**, *53*, 7.
35. Han, X. *Tetrahedron Lett.* **2010**, *51*, 360.
36. Maestro, V10.5; Schrödinger, Inc.: Portland, OR, 2014.

Graphical Abstract

To create your abstract, type over the instructions in the template box below.
Fonts or abstract dimensions should not be changed or altered

Selectivity switch between FAK and Pyk2: Macrocyclization of FAK inhibitors improves Pyk2 potency

Leave this area blank for abstract info.

Julie Farand, Nicholas Mai, Jayaraman Chandrasekhar, Zachary E. Newby, Josh Van Veldhuizen, Jennifer Loyer-Drew, Chandrasekar Venkataramani, Juan Guerrero, Amy Kwok, Ning Li, Yelena Zherebina, Sibylle Wilbert, Jeff Zablocki, Gary Phillips, William J. Watkins, Robert Mourey, Gregory Notte